

Many-qutrit Mermin inequalities with three measurement settings

Jay Lawrence

Department of Physics and Astronomy,

Dartmouth College, Hanover, NH 03755, USA and

The James Franck Institute, University of Chicago, Chicago, IL 60637

(Dated: revised February 3, 2022)

Abstract

Mermin inequalities are derived for systems of three-state particles (qutrits) employing three local measurement settings. These establish perfect correlations which violate local realistic bounds more strongly than those previously reported with two bases. The quantum eigenvalue of this Mermin operator grows as the dimension of the Hilbert space, 3^N , rather than 2^N , as obtained with two bases. The number of distinct GHZ contradictions also increases as 3^N .

PACS numbers: 03.67-a, 03.65.Ta, 03.65.Ud

I. INTRODUCTION

This work is motivated by recent experimental breakthroughs on the entanglement of three nonbinary particles [1, 2]. In particular, a three-qutrit GHZ state has recently been produced and documented for the first time [2]. The qutrits are realized with photon orbital angular momentum, and years of progress leading to the present breakthroughs are reviewed in Ref. [3]. Here we build upon a recent theoretical calculation for qutrits [4] by extending the number of local measurement settings from two to three, equal to the number of outcomes. This extension enhances the violations of local realism qualitatively.

Such violations are expressed by Greemberger-Horne-Zeilinger (GHZ) paradoxes [5], or by Bell inequalities [6, 7]. In this work we choose a special form of the latter, called Mermin inequalities, because they reveal individual GHZ contradictions implicitly, as pointed out in Mermin’s original work [8, 9]. The Mermin *operator* is a sum of N -particle tensor products, each of which has the same given state as an eigenstate, with the same eigenvalue. Hidden variables can duplicate this eigenvalue for a subset of these tensor products, but are thereby constrained to predict different values for others. This gives rise to specific GHZ contradictions as well as to violations of the Mermin inequality itself, which places an upper bound on the hidden variable value of the Mermin operator. A Mermin inequality has been defined formally by Cabello et. al. [10], as a Bell inequality (I) whose “Bell operator is a sum of stabilizing operators” that represent the perfect correlations in their simultaneous eigenstate, and (II) which maximizes the violations for that state. Here as in [4], we have taken this definition to include *concurrent* operators [11], which do not commute but share a common eigenstate - these were essential to the discovery of GHZ contradictions [12, 13] and Mermin inequalities [4] for qutrits. This work shows that concurrent operators built from three local measurement settings achieve an eigenvalue growth rate $\sim 3^N$, the appropriate analog to Mermin’s $\sim 2^N$ for qubits, achieved with commuting stabilizers.

A brief review of general developments since GHZ [5] and Mermin [8] was given in Ref. [4] and won’t be repeated here. But we should emphasize, for the sake of comparison, that Bell inequalities have been developed which serve as criteria for *irreducible* N -particle entanglement - so that violations for a given state rule out its factorization into any subsets of fewer than all N particles [14, 15]. A relevant example is a recent treatment of qutrit systems [16] in which, as here, three measurement settings were used. The Bell operators

are more complex and require separate analyses for different numbers of particles. Qutrit results are presented for the cases of $N = 2 - 6$. As expected from earlier examples, the violations of this type of Bell inequality grow more slowly with N than the violations of Mermin inequalities.

In the next section we describe a set of related GHZ states and the rotationally covariant observables that comprise the Mermin operator, and we compare its quantum and classical values. The quantum values will be obvious, but the classical maxima require proof, and this is spelled out in Section III. In the concluding section, we discuss the physical significance of our results, including a count of GHZ contradictions, and we comment on higher dimensional systems.

II. THE MERMIN OPERATOR - QUANTUM AND CLASSICAL VALUES

To construct the Mermin operator, first consider the nine related N -qutrit GHZ states,

$$|\Psi_k\rangle = \frac{1}{\sqrt{3}}(|00\dots 0\rangle + \alpha^k|11\dots 1\rangle + \alpha^{2k}|22\dots 2\rangle), \quad (k = 0, 1, \dots, 8), \quad (1)$$

where $\alpha = \exp(2\pi i/9)$, so that each $|\Psi_k\rangle$ is generated from $|\Psi_0\rangle$ by a rotation through $2\pi k/9$, as shown in Fig. 1a. It is a defining symmetry of GHZ states [13] that such rotations may be distributed arbitrarily among qutrits (about their respective \hat{z} axes), in increments that add up to the net rotation angle.

Next consider an observable of which $|\Psi_0\rangle$ is an eigenstate with eigenvalue unity,

$$\mathbf{X} \equiv X^{\otimes N} = X_1 \dots X_N. \quad (2)$$

Its factors are the standard qutrit Pauli matrices, $X_i = \sum_{n=0}^2 |n+1\rangle_i \langle n|_i$, acting on the i th qutrit. Rotations of these factors through the basic angles ($\pm 2\pi/9$) generate other qutrit matrices which we call, respectively (dropping the index i),

$$Y \equiv Z^{1/3} X Z^{-1/3} = \sum_{n=0}^2 |n+1\rangle \alpha^{(1-3\delta_{n,2})} \langle n|, \quad (3)$$

$$V \equiv Z^{-1/3} X Z^{1/3} = \sum_{n=0}^2 |n+1\rangle \alpha^{(3\delta_{n,2}-1)} \langle n|; \quad (4)$$

where $Z = \sum_{n=0}^2 |n\rangle \omega^n \langle n|$ is the usual diagonal Pauli matrix, which rotates qutrits through $2\pi/3$ about \hat{z}_i . Given X , Y , and V factors for each qutrit, we construct the 3^N tensor product operators in which each factor can be X or Y or V . Every such tensor product

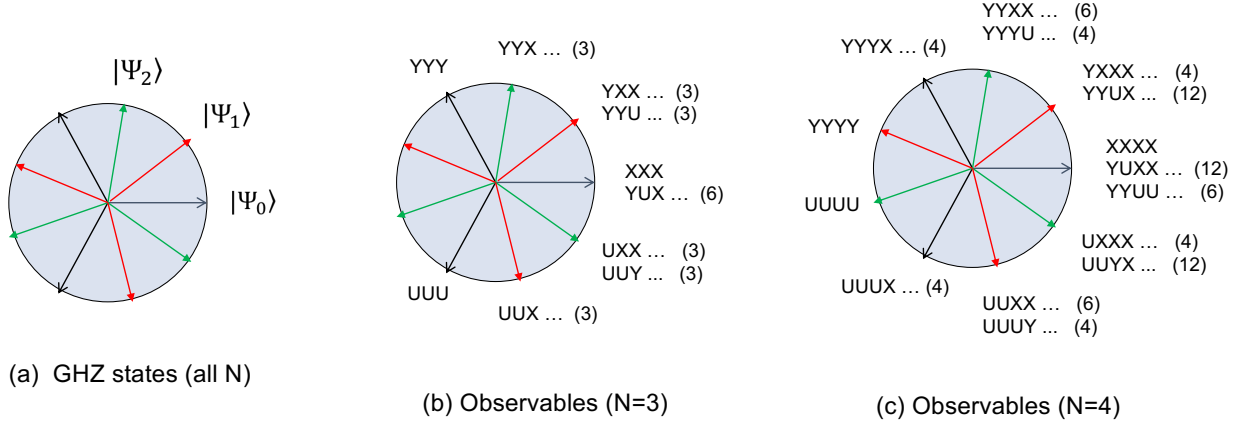


FIG. 1: (a) GHZ states (Eq. 1), and (b) tensor product observables for $N = 3$ and (c) $N = 4$. Parentheses denote the number of permutation-related tensor products. Black arrows define the subset whose joint eigenstate is $|\Psi_0\rangle$. Red and green arrows relate similarly to $|\Psi_1\rangle$ and $|\Psi_2\rangle$.

is generated from \mathbf{X} by some combination of one-qutrit rotations (through 0 or $\pm 2\pi/9$, respectively), and Figs. 1(b and c) show the net rotations for $N = 3$ and 4. Because of rotational covariance, all operators at point k share the state $|\Psi_k\rangle$ as an eigenstate with eigenvalue unity.

Now, operators have a periodicity property [13] - a rotational Bloch theorem: If any factor (X , Y , or V) is rotated through $2\pi/3$, it is simply multiplied by ω ; that is, $ZXZ^{-1} = \omega X$, and similarly for Y and V . This means that ωXXX (like YYY) appears at the point 3 (rotation angle $2\pi/3$), and it follows that every operator at point 3 has $|\Psi_0\rangle$ as an eigenstate *with eigenvalue* ω . Similarly, every operator at point 6 has $|\Psi_0\rangle$ as an eigenstate with eigenvalue ω^2 . Therefore, we may define the Mermin operator for the state $|\Psi_0\rangle$ as

$$\begin{aligned} \mathcal{M}_0 = & (\text{sum of operators at } k = 0) \\ & + \omega^2(\text{sum of operators at } k = 3) + \omega(\text{sum of operators at } k = 6), \end{aligned} \quad (5)$$

which includes all operators identified by black arrows in Fig. 1, and in which every term contributes +1 to the eigenvalue, so that

$$\mathcal{M}_0|\Psi_0\rangle = 3^{N-1}|\Psi_0\rangle. \quad (6)$$

One could define different Mermin operators, \mathcal{M}_1 and \mathcal{M}_2 , corresponding to $|\Psi_1\rangle$ and $|\Psi_2\rangle$ and identified by red and green arrows, respectively. These have identical eigenvalues because

TABLE I: Quantum eigenvalues, \mathcal{M}_Q , classical upper bounds, \mathcal{M}_C , and their ratio, \mathcal{R} , for N qutrits. We also list the number of distinct GHZ contradictions which may be constructed from terms appearing in the Mermin operator.

N	\mathcal{M}_Q	\mathcal{M}_C	\mathcal{R}	\mathcal{N}_{GHZ}
3	9	6	1.5	2
4	27	15	1.8	8
5	81	36	2.25	30
6	243	90	2.70	102
7	729	225	3.24	336

each accounts for one-third of all operators appearing on the plot. We focus on \mathcal{M}_0 because its higher symmetry simplifies the analysis.

Let us briefly compare the above quantum result with the classical, or hidden variable result. The assumption embodying local realism, or noncontextuality, is that every local factor, X_i, Y_i, V_i , takes a definite value [eg, $v(X_i) = 1, \omega$, or ω^2], and it must take the same value wherever it appears. A given choice produces a classical value of the Mermin operator, $v(\mathcal{M}_0)$. Our goal is to find its maximum absolute value, $|v(\mathcal{M}_0)|$, over all such choices, which we call \mathcal{M}_C . We shall simply state here (and prove in the following section) that the maximum is realized when all local factors take the same value (eg., unity). Then, Eq. 5 reduces to

$$\begin{aligned}
& \mathcal{M}_C = (\text{number of operators at } k = 0) \\
& + \omega^2(\text{number of operators at } k = 3) + \omega(\text{number of operators at } k = 6) \\
& = (\text{number of operators at } k = 0) - (\text{number of operators at } k = 3 \text{ or } 6), \quad (7)
\end{aligned}$$

where $\omega^2 + \omega = -1$ and the equality of numbers at $k = 3$ and 6 was used. The resulting values are compared in Table I with the quantum eigenvalue, $\mathcal{M}_Q = 3^{N-1}$.

Each violation of Mermin's inequality (ratio $\mathcal{R} \equiv \mathcal{M}_Q/\mathcal{M}_C > 1$) reflects many specific GHZ contradictions (or paradoxes), which may be extracted from Tables 1b,c and their larger- N generalizations. Reference [13] shows that HV assignments respecting the (common) eigenvalue of a subset of operators at the $k = 0$ point predict the wrong value for any

operator at point 3 or point 6 [17]. The number of distinct GHZ contradictions is equal to the number of wrong predictions, so that

$$\mathcal{N}_{GHZ} = (\text{number of operators at } k = 3 \text{ and } 6) = \frac{2}{3}(\mathcal{M}_Q - \mathcal{M}_C), \quad (8)$$

as illustrated in Table I. The second equality follows from Eqs. 5 - 7. A detailed discussion of these and similar GHZ contradictions will be given elsewhere.

III. PROOF OF CLASSICAL MAXIMA

We now prove that Eq. 7 indeed provides the maximum hidden variable value of \mathcal{M}_0 , and we derive a closed-form expression. We begin by showing that the Mermin operator is given by the identity,

$$\begin{aligned} \mathcal{M}_0 = \frac{1}{3} \Bigg[& \bigotimes_{i=1}^N (X_i + \alpha^2 Y_i + \alpha^{-2} V_i) + \bigotimes_{i=1}^N (X_i + \omega \alpha^2 Y_i + \omega^2 \alpha^{-2} V_i) \\ & + \bigotimes_{i=1}^N (X_i + \omega^2 \alpha^2 Y_i + \omega \alpha^{-2} V_i) \Bigg]. \end{aligned} \quad (9)$$

To verify, note that each product generates a weighted sum of all 3^N operators shown on the circle graph. Then, using $\omega^2 + \omega + 1 = 0$, one can show that a given term survives in the sum only if the number of Y factors equals the number of V factors mod. 3. This locates surviving terms at the black arrows in Fig. 1. Finally, using $\alpha^3 = \omega$, one can show that the multiplying factors of these terms are just those given by Eq. 5. Thus, 9 is equivalent to 5.

We shall evaluate the HV value, $v(\mathcal{M}_0)$, directly from 9. $v(\mathcal{M}_0)$ is a function of the values, $v(X_i)$, etc., assigned to each local factor. But its magnitude, $|v(\mathcal{M}_0)|$, depends only on two independent local ratios, which we choose to be

$$R_i = v(Y_i)/v(X_i) \quad \text{and} \quad S_i = v(V_i)/v(X_i). \quad (10)$$

We then have

$$\begin{aligned} |v(\mathcal{M}_0; R_i, S_i)| = \frac{1}{3} \Bigg| & \bigotimes_{i=1}^N (1 + \alpha^2 R_i + \alpha^{-2} S_i) + \bigotimes_{i=1}^N (1 + \omega \alpha^2 R_i + \omega^2 \alpha^{-2} S_i) \\ & + \bigotimes_{i=1}^N (1 + \omega^2 \alpha^2 R_i + \omega \alpha^{-2} S_i) \Bigg| \end{aligned} \quad (11)$$

$$\equiv \frac{1}{3} \Bigg| \bigotimes_{i=1}^N \mathcal{B}(R_i, S_i) + \bigotimes_{i=1}^N \mathcal{C}(R_i, S_i) + \bigotimes_{i=1}^N \mathcal{A}(R_i, S_i) \Bigg|, \quad (12)$$

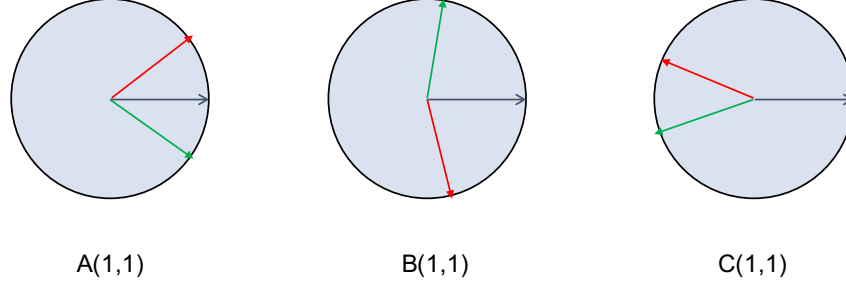


FIG. 2: Complex contributions to each of the real numbers A , B , and $-C$ appearing in Eqs. 13 - 15, respectively. Phase angles are color-coded as in Fig. 1.

where the last line simply assigns names to the individual qutrit factors in the expression above. These names are chosen because, when evaluated at $R_i = S_i = 1$ (the “uniform HV” point), the sums become

$$\mathcal{A}(1, 1) = (1 + \omega^2 \alpha^2 + \omega \alpha^{-2}) = 1 + 2 \cos \frac{2\pi}{9} \equiv A \approx 2.532, \quad (13)$$

$$\mathcal{B}(1, 1) = (1 + \alpha^2 + \alpha^{-2}) = 1 + 2 \cos \frac{4\pi}{9} \equiv B \approx 1.347, \quad (14)$$

$$\mathcal{C}(1, 1) = (1 + \omega \alpha^2 + \omega^2 \alpha^{-2}) = 1 + 2 \cos \frac{8\pi}{9} \equiv -C \approx -0.879; \quad (15)$$

their magnitudes are ordered as $A > B > C > 0$, with $C(1, 1) \equiv -C$ being negative. The three complex contributions to each of A , B , and $-C$ are shown in Fig. 2.

The hidden variable magnitude of \mathcal{M}_0 at this “uniform HV” point is given by

$$|v(\mathcal{M}_0; 1, 1)| = \frac{1}{3}(A^N + B^N \pm C^N), \quad \text{for } N \text{ even/odd}, \quad (16)$$

which duplicates the results of Eq. 7 and Table I. We now show that this expression gives the maximum possible value of $|v(\mathcal{M}_0; R_i, S_i)|$ for all $N \geq 3$.

As background, Table II shows how the hidden variable choices (R and S) affect the individual qutrit factors appearing in Eq. 12. To derive Table II, observe that the choices $R = \omega$ (ω^2) correspond, in Fig. 2, to rotations of each *green* arrow by 120° (-120°), while $S = \omega$ (ω^2) correspond to rotations of each *red* arrow by 120° (-120°). All entries follow immediately. Two entries are pure rotations in the complex plane. Two others are pure cyclic permutations. The remaining four are combinations of both. But note that every choice preserves the total number of times (N) that each factor (A , B , C) appears in the *sum* in Eq. 12. So, under an arbitrary set of HV assignments (R_i, S_i), expression 16 will be modified by a reshuffling of these factors among the three terms, preserving the total

TABLE II: Dependence of single-qudit factors $\mathcal{A}(R_i, S_i)$, etc., on hidden variable choices. A , B , and C are real positive numbers (Eqs. 13 - 15), and phase angles are given in degrees where needed.

R	S	$\mathcal{A}(R, S)$	$\mathcal{B}(R, S)$	$\mathcal{C}(R, S)$
1	1	A	B	$-C$
ω	1	$A(40^\circ)$	$B(-80^\circ)$	$C(-20^\circ)$
1	ω^2	$A(-40^\circ)$	$B(80^\circ)$	$C(20^\circ)$
ω	ω^2	B	$-C$	A
ω^2	ω	$-C$	A	B
ω^2	1	$C(20^\circ)$	$A(-40^\circ)$	$B(80^\circ)$
1	ω	$C(-20^\circ)$	$A(40^\circ)$	$B(-80^\circ)$
ω	ω	$B(80^\circ)$	$C(20^\circ)$	$A(-40^\circ)$
ω^2	ω^2	$B(-80^\circ)$	$C(-20^\circ)$	$A(40^\circ)$

number of each factor; and a rotation of each term in the complex plane. From this alone, it is clear that expression 16, for *even* N , gives the maximum of $|v(\mathcal{M}_0, R_i, S_i)|$ over all hidden variable choices.

The odd N case requires further discussion: We must show that no HV assignment can realign the C^N term without a compensating reduction of $A^N + B^N$. It is easy to show this for any assignment producing a net permutation. For example, in the case of $N = 3$, no such trial value $|v(\mathcal{M}_0, R_i, S_i)|$ can exceed $A^2B + B^2C + C^2A \approx 4.06$, which is less than $A^3 + B^3 - C^3 = 6$. The failure is more dramatic for larger N , for any set of one-qudit permutations that does not include all of the particles (which simply reproduces the maximum value).

It remains to consider the pure rotations. Table II shows that there are two possible outcomes: The A^N and B^N terms can either be aligned (zero relative phase), or not (relative phases $\pm 120^\circ$). The latter case is clearly ruled out. In the former case, the C^N term is always oppositely aligned for odd N , so that Eq. 16 indeed represents the maximum value, $|v(\mathcal{M}_0; 1, 1)| = \mathcal{M}_{HVM}$, for all N .

It is clear from Eq. 16 that the large- N asymptote is $\mathcal{M}_C \rightarrow \frac{1}{3}(2.532)^N$, so that the

TABLE III: Mermin eigenvalue \mathcal{M}_Q compared with the dimension \mathcal{D} of the Hilbert space. d is the particle dimension and s is the number of measurement settings.

source	d	s	\mathcal{M}_Q	\mathcal{D}
qubits (Ref. [8])	2	2	2^{N-1}	2^N
qutrits (Ref. [4])	3	2	$2^N/3$	3^N
qutrits (present)	3	3	3^{N-1}	3^N

quantum to classical ratio increases as

$$\lim_{N \rightarrow \infty} (\mathcal{M}_Q/\mathcal{M}_C) \approx (3/2.532)^N \approx 1.185^N, \quad (17)$$

as compared with 1.064^N when two measurement settings are used. Also note that the divergence of this ratio shows that Eq. 8 reduces, asymptotically, to

$$\lim_{N \rightarrow \infty} (\mathcal{N}_{GHZ}/\mathcal{M}_Q) = 2/3. \quad (18)$$

IV. CONCLUSIONS

We have derived many-qutrit Mermin inequalities employing three measurement settings. The effect of this extension is shown in Table III, which compares the qutrit cases (two *vs* three settings), with Mermin's original qubit proof [8]. In the two cases where the number of independent measurement settings (s) is equal to the particle's dimension d , the quantum value \mathcal{M}_Q grows as the dimension \mathcal{D} of the Hilbert space of the system. It is well known that $\mathcal{D} - 1$ is the number of operators which can be diagonalized simultaneously. It is also the number of operators which can share a common eigenstate. So \mathcal{M}_Q , the number of operators which contribute to \mathcal{M}_0 , grows as a fixed fraction of the total number that can take sharp values simultaneously. In the qubit case, $\mathcal{M}_Q = \mathcal{D}/2$, while in the qutrit case, $\mathcal{M}_Q = \mathcal{D}/3$. The same is true, asymptotically, for the number of distinct GHZ contradictions, where $\mathcal{N}_{GHZ} \rightarrow \mathcal{D}/4$ for qubits [18], while $\mathcal{N}_{GHZ} \rightarrow 2\mathcal{D}/9$ for qutrits (Eq. 18).

The symmetry of the construction in Fig. 1 extends to systems of higher odd dimensions, provided that $s = d$ independent settings are used. On this basis, for $d = 5$, we would expect the quantum value $\mathcal{M}_Q = 5^{(N-1)} = \mathcal{D}/5$, although the hidden variable maximum is

less clear-cut. Supposing that the optimal HV assignment is the uniform one, we could guess the asymptotic classical maximum to be $\mathcal{M}_C \approx 4.6898^N/5$, so that the quantum violation of this bound grows as $\mathcal{R} \approx 1.066^N$.

There are daunting practical limitations to preparing entangled systems with larger d as well as larger N . Regarding fundamental limitations, however, there is no limit on N , while increasing d narrows the quantum-classical gap (\mathcal{R}). The narrowing found here suggests that hidden variables can better mimic the quantum values as d increases.

-
- [1] M. Malik, M. Erhard, M. Huber, M. Krenn, R. Fickler, and A. Zeilinger, *Nature Photonics*, **10**, 248 (2016).
 - [2] M. Erhard, M. Malik, M. Krenn, and A. Zeilinger, *Nature Photonics*, **12**, 759 (2018).
 - [3] M. Erhard, R. Fickler, M. Krenn, and A. Zeilinger, *Light: Science and Applications*, **7**, 17146 (2018).
 - [4] J. Lawrence, *Phys. Rev. A* **95**, 042123 (2017).
 - [5] D.M. Greenberger, M.A. Horne, and A. Zeilinger, in *Bell's Theorem, Quantum Theory and Conceptions of the Universe*, edited by M. Kafatos (Kluwer Academic, Dordrecht, 1989), p. 69, and eprint arXiv:quant-ph/0712.0921(2007).
 - [6] J. S. Bell, *Physics* **1**, 195 (1964).
 - [7] J.F. Clauser, M.A. Horne, A. Shimony, and R.A. Holt, *Phys. Rev. Lett.* **23**, 880 (1969).
 - [8] N. D. Mermin, *Phys. Rev. Lett.* **65**, 1838 (1990).
 - [9] In GHZ paradoxes, the local observables acquire the status of elements of reality, as defined by A. Einstein, B. Podolsky, and N. Rosen, *Phys. Rev.* **47**, 777 (1935).
 - [10] A. Cabello, O. Gühne, and D. Rodríguez, *Phys. Rev. A* **77**, 062106 (2008).
 - [11] J. Lee, S.-W. Lee, and M.S. Kim, *Phys. Rev. A* **73**, 032316 (2006) employed concurrent observables to find GHZ paradoxes in all even d and odd N systems. To my knowledge, this marked their first usage in such proofs.
 - [12] J. Ryu, C. Lee, M. Zukowski, and J. Lee, *Phys. Rev. A* **88**, 042101 (2013).
 - [13] J. Lawrence, *Phys. Rev. A* **89**, 012105 (2014).
 - [14] Svetlichny, *Phys. Rev. D* **35**, 3066 (1987).
 - [15] D. Collins, N. Gisin, S. Popescu, D. Roberts, and V. Scarani, *Phys. Rev. Letters* **88**, 170405

- (2002).
- [16] D. Alsina, A. Cervera, D. Goyeneche, J. I. Latorre, and K. Zyczkowski, *Phys. Rev. A* **94**, 032102 (2016).
 - [17] Methods developed in Ref. [13] all spring from the point made in the subsection “general failure of hidden variables,” on pp. 3 and 4.
 - [18] J. Lawrence, eprint arXiv: quant-ph/0506063v.1 (2005) works this number out for qubits.